INDERSCIENCE PUBLISHERS
Linking academia, business and industry through research

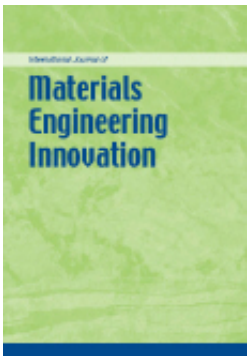


**International Journal of Materials Engineering Innovation**

ISSN online: 1757-2762 - ISSN print: 1757-2754
https://www.inderscience.com/ijmatei

# Study of substitution of carburised 16MnCr5 used in sub-axis of machine tool spindle by carbonitrided steel

Mir Nariman Yoozbashi

**DOI:** 10.1504/IJMATEI.2022.10047997

**Article History:**

| | |
|---|---|
| Received: | 31 October 2021 |
| Accepted: | 18 January 2022 |
| Published online: | 16 January 2023 |

*Copyright © 2023 Inderscience Enterprises Ltd.*

# Study of substitution of carburised 16MnCr5 used in sub-axis of machine tool spindle by carbonitrided steel

Mir Nariman Yoozbashi

University of Applied Science and Technology,
End of Taleghani Street, Tabriz, IR, Iran
Fax: +98-41-35430403
Email: n.yoozbashi@uast.ac.ir
Email: nariman_yoozbashi@yahoo.com

**Abstract:** The focus of the current study is using carbonitrided 16MnCr5 instead carburised steel in the sub-axis of machine tool spindles by investigation on the impact fracture toughness and fatigue strength of 16MnCr5 steel. Samples after preparation were surface treated by carburising and carbonitriding treatments. The characteristics of toughness and fatigue were presented through impact test and rotating bending fatigue machine. To clarify toughness variation mechanisms, and relation with microstructure, observations of microstructure and fracture surfaces carried out by optical microscopy and scanning electron microscopy. Microhardness tests and roughness were evaluated by using equipment. The experimental results showed that, carburised and carbonitrided specimens are relatively similar in properties such as microstructure feature and how to fracture and differ in properties such as hardness distribution, depth of hardened layer, impact energy and roughness. In general, it can be claimed that in the spindle sub-axis, carbonitriding treatment is a good alternative to carburising.

**Keywords:** 16MnCr5; carburising; carbonitriding; spindle; microstructure; mechanical properties.

**Reference** to this paper should be made as follows: Yoozbashi, M.N. (2023) 'Study of substitution of carburised 16MnCr5 used in sub-axis of machine tool spindle by carbonitrided steel', *Int. J. Materials Engineering Innovation*, Vol. 14, No. 1, pp.79–93.

**Biographical notes:** Mir Nariman Yoozbashi received his MSc degree in Materials Characterisation and Selection in 2006 and a PhD degree in Materials Engineering in 2011 from the Sahand University of Technology, Islamic Republic of Iran. He currently works as an Assistant Professor at the University of Applied Science and Technology of Iran. His current research interests include the mechanical and microstructural properties, production and heat treatment of steels. Also, he currently serves as the President of University of Applied Science and Technology of Province of Zanjan of Iran.

Copyright © 2023 Inderscience Enterprises Ltd.

## 1 Introduction

Spindle as one of the important components of computer numerical control (CNC) machines, have a major effect on metal removal rates and quality of the machined parts (Abele et al., 2010). Because of their inherent benefits, many machine tool manufactures around the world recommended high speed spindles, some at speeds of around 100,000 rpm (Altintas and Cao, 2005; Li and Shin, 2004). The rough machining of a steel is characterised by high cutting forces, moments and medium rotational speeds. In those situations, larger spindles and larger diameter bearings are required to withstand the loads (Brecher et al., 2007). High speed spindle machine vibration factors that affect machining accuracy include tool holders, tools and spindle (Cao and Altintas, 2007).

In the spindle, the sub-axis is used as a rotating to fix the tool or workpiece, has been marked with a green loop in the Figure 1. According to the information achieved from the machine tool company, 16MnCr5 steel in carburised condition used as a sub-axis of spindle. Machine parts such as axis, gears and cams often require a very hard surface that is resistant to abrasion and a soft and tough core that can withstand impact loads. A straightforward method of providing a combination of hard surface and soft core is surface hardening of steel using carburisation and subsequent quenching (Mohan and Arul, 2018; Yeğen and Usta, 2010; Davis, 2002).

**Figure 1** An experimental of machine tool spindle; shaft of spindle is marked with a green loop (see online version for colours)

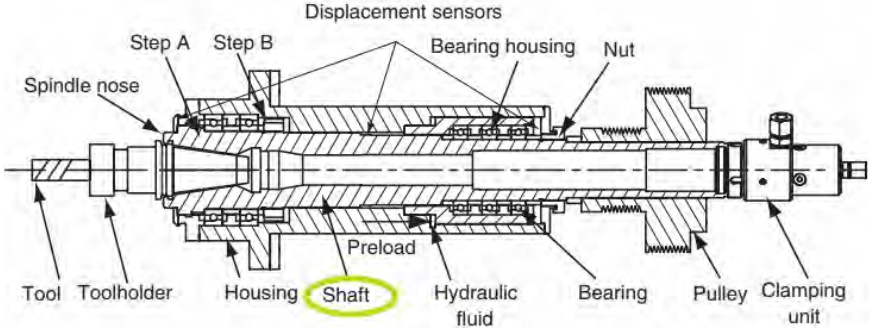


*Source:* Cao and Altintas (2007)

It is essential to have a combination of suitable fatigue strength and high fracture toughness to increase the range of applied load and safety factor in engineering structures (Putatunda, 2001). Fracture toughness is an important material property in fracture prevention (Hertzberg et al., 2020; Oropeza, 2002). Failure of metals by fatigue results from loads which are varied or repeated (Forrest, 2013). Fatigue strength can be significantly improved by surface treatment such as nitriding and carburising. Up to 91% enhancement of fatigue limit by using of ion nitriding has been reported by Sirin et al. (2008). Significant possibilities for increasing the fatigue strength, with about 80%, were observed during ion nitration of 0.42% C, Cr-alloyed steel (Tchankov and Dimitrov, 2000). Wear resistance of the specimens has been increased by the cementation processes (Yeğen and Usta, 2010). The thermal fatigue strength of samples operated by laser is considerably higher than as-received condition (Zhang et al., 2013). Surface roughness increasing by nitriding can be related to the growth of $\varepsilon$-nitrides on the surfaces of the

steel (Badisch et al., 2016). Fatigue strength of specimens has been improved by about 14%, under the applying of shot peening, while decreasing about 8% occurred by double stage nitriding. Fatigue strength decreasing has been occurred about 29% and 50% by nitrocarburising and single stage nitriding, respectively (Farrahi and Ghadbeigi, 2006). Nucleation of the cracks in the surface-treated specimens always occurs at the interface between the carburised case and the core (Ceschini and Minak, 2008). Hardness of the surface and fatigue limit has been increased by 385% and 23.76% at two million cycles by nitriding (Winck et al., 2013). The results by Dastmozd et al. (2014) showed that the wear behaviour of the steel has been improved by applying surface heat treatments. Yoozbashi and Almasi (2018) have shown that carbonitriding has a larger effect on wear behaviour compared to the other surface treatments consisting of carburising, nitriding and nitrocarburising, Also, Yoozbashi et al. (2017) have imported the effects of the tempering on wear properties of 16MnCr5 used in high-speed spindle.

The focus of the current study was using carbonitrided 16MnCr5 instead carburised steel in machine tool spindles by investigation the impact fracture toughness and fatigue strength of 16MnCr5 steel. Success in this work will allow the use of different materials, longer work life of pieces, greater mechanical properties and customer satisfaction. The surface treatments cycle used in this study, have been selected according to the works of Yoozbashi and Almasi (2018) which showed the better wear resistance among the selected cycles.

## 2 Experimental details

The study was performed on the 16MnCr5 steel in the normalised state. Chemical composition of this steel is given in Table 1. The standard Charpy V-notch specimens and fatigue test samples were provided according to the requirements of American Society for Testing and Materials (2013) and DIN 50 113 (2018) standards test method of metallic materials, as shown in Figure 2.

**Table 1** Chemical composition of the normalised 16MnCr5 steel

| Element | C | Si | Mn | P | S | Cr |
|---|---|---|---|---|---|---|
| Content (wt. %) | 0.17 | 0.4 | 1.15 | 0.03 | 0.02 | 0.95 |

**Figure 2** Dimensions of samples of, (a) Charpy V-notch impact test (b) rotating bending fatigue test (see online version for colours)

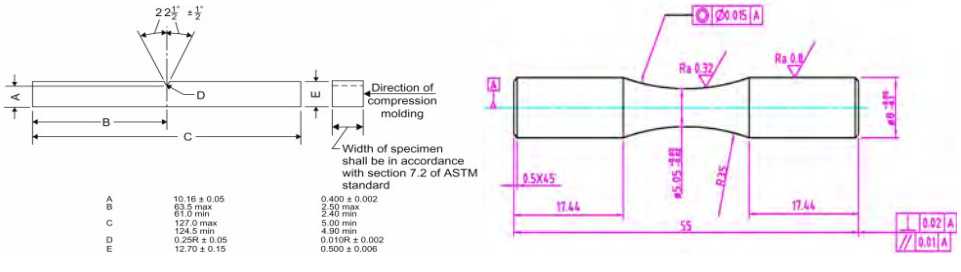


(a) (b)

The samples were subjected to surface heat treatment processes. First series of samples preheated at 550°C for two hours; then carburising was carried out at 920°C for five hours in a gaseous atmosphere containing Co and $CH_4$ and air cooled. After that, the samples were austenitisied at 840°C for 30 min and followed by rapid cooling with quenching in oil. Eventually, to investigate the effects of tempering temperatures on impact toughness, samples were tempered at temperatures of 100, 150, 200 and 250°C for one hour. Samples of this series were named with carburised specimens (CS).

Second series of samples preheated at 550°C for 2 h; then carbonitrided at 880°C for five hours in a gaseous atmosphere containing 60% air, 20% ammonia and 20% liquefied petroleum gas (LPG) with a gas pressure of input 1 bar and quenched in oil. Finally, tempering of impact toughness samples were done at temperatures of 100, 150, 200 and 250°C for 1 h. Samples of this series were named with carbonitrided specimens (CNS).

According to the impact test results to determine the optimal heat treatment condition, tempering of fatigue samples was done at this condition.

The fracture toughness tests were carried-out using a Roell Amsler RKP 300 impact test machine at room temperature. For each condition of tempering treatments, three samples have been used for toughness measurements. The rotating bending fatigue tests were performed by Roell Amsler UBM 200 equipment at 2,800 rpm in laboratory conditions. For each stress level, two to three samples were tested and subsequent samples were tested in applied stress. Observations of microstructure and fracture surfaces carried out by optical microscopy (OM) and scanning electron microscopy (SEM). A micro Vickers hardness test was used to determine the hardness of specimens. A load of 100 gf was used to measure the hardness of samples. An MAHRTM equipment was employed to evaluate the surface roughness of the samples.

## 3 Results and discussion

As mentioned earlier, to increase the range of applied load and safety factor in engineering structures, it is needed to have a combination of suitable fatigue strength and high fracture toughness. Therefore, in the current study, the CS and CNS will be compared from the perspectives of impact toughness and fatigue strength. Also, other properties such as hardness distribution, microstructure and how to fracture of CS and CNS will be discussed.

### *3.1 Hardness distribution and microstructure of the CS and CNS*

The hardness variations of CS and CNS as a function of tempering temperature are shown in Figure 3. It can be seen, with increasing of the tempering temperature, the hardness values reduces, which could be reasonably explained by the effects of tempering temperature. The microstructure of the steel tempered at lower temperature is mainly consisted of tempered martensite and a small amount of carbides. Tempering of the steel at the Lower temperature, also, leads to extremely low carbon diffusion and retardation of the formation of ferrite and cementite from martensite. Therefore hardness values are higher at the lower tempering temperatures. When the steel is tempered at higher temperature, the size of carbides increases obviously, and formation of ferrite and cementite from martensite accelerated, eventually the hardness decreases greatly.

**Figure 3** Hardness variations as a function of tempering temperatures for CS and CNS

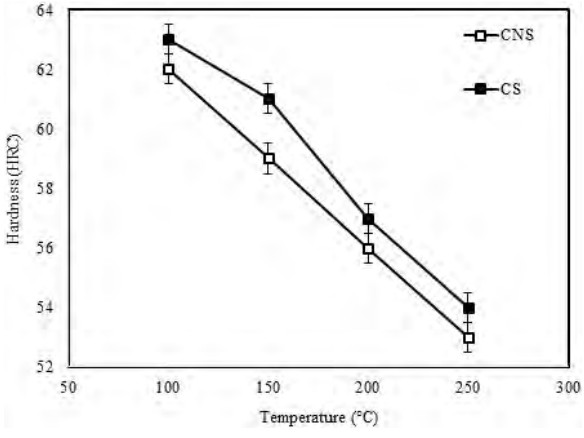


**Figure 4** 16MnCr5 steel microhardness graph after various surface treatments, (a) CS (b) CNS

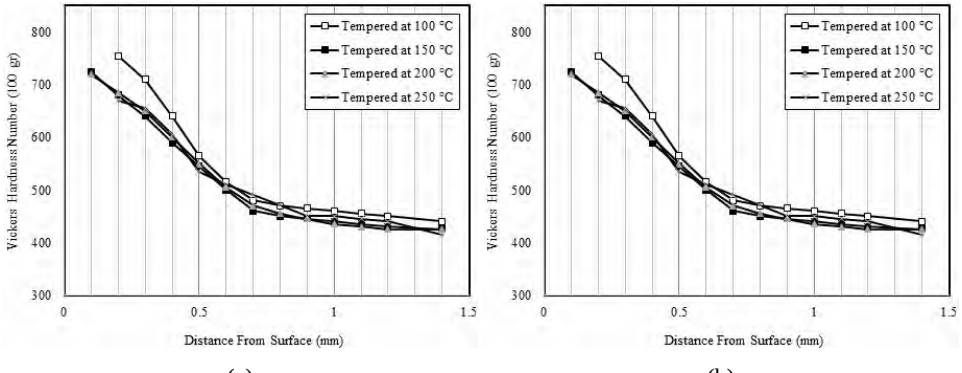


(a) (b)

As shown in the figure, carburised 16MnCr5 steel shows the higher hardness value than that of carbonitrided one. After carburising, the formation of carbide compounds such as manganese and chromium carbides increases the hardness compared to the CNS.

The chemical composition of the surfaces of CS and CNS consists of Mn, Cr, Mo and Cr alloying elements that provides the higher hardenability. As a result, higher increase of hardness has been occurred during surface treatment. The hardness of the 16MnCr5 steel in raw condition revealed about 150 VHN.

According to the nature of martensitic transformation and the change in the chemical composition of the specimen surface; the increase of surface hardness is predictable to certain intervals of the surface and it can be analysed by using the results of microhardness distribution.

Figure 4 shows the microhardness variations as a function of distance from surface after different tempering temperature. It implies that hardened layers have been formed at the surface of the specimens. The hardness of CS and CNS has decreased from the surface to the core of specimens depending on the carbon profile that reaches maximum content at surface and decreases in the core. The core hardness of CS increased by the quench process performed after the carburising.

The comparison of harness variations of CS and CNS tempered at 200°C have been shown in Figure 5. It can be seen that the hardness distribution of CS located at higher level compared to that of CNS. This is in agreement with the results given in Figure 3. With considering the hardness criterion of 550 VHN (Krauss, 2015), depth of the hardened layer of CS and CNS, has been given in the Table 2. It can be seen that, depth of hardened layer of CS is higher compared to the CNS. This can be as a result of higher temperature of treatment of CS than CNS. Carbonitriding alters only the top layers of the workpiece and maximum case depth is typically restricted to 0.75 mm. Also, lower hardness of CS at the surface can be due to the decarburisation of these specimens during surface treatment.

**Figure 5** 16MnCr5 steel microhardness graph for CS and CNS tempered at 200°C

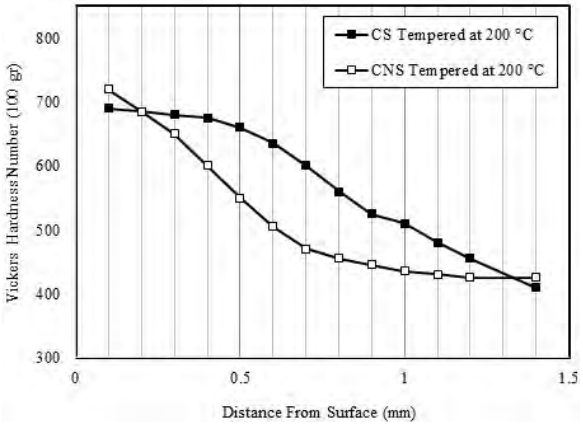


**Table 2** Depth of hardened layer of CS and CNS for different tempering temperatures

| Tempering temperature (°C) | 100 | 150 | 200 | 250 |
|---|---|---|---|---|
| Depth of hardened layer of CS (mm) | 0.8 | 0.92 | 0.83 | 0.6 |
| Depth of hardened layer of CNS (mm) | 0.53 | 0.49 | 0.5 | 0.38 |

Figures 6 and 7 show optical micrographs of the surface regions of the CS and CNS. As it can be seen, the surface microstructure of specimens has undergone some changes due to carburising and carbonitriding. It is obvious that the size of the microstructure components are similar in the CS and CNS. Figures, also, show that, the microstructure involving of aggregates of tempered martensite (dark and brown etched areas) and retained austenite (white areas). These figures show a lower retained austenite in the microstructures. The retained austenite regions exhibit two different morphologies; thin films and blocks. The thin films of retained austenite contains higher level of carbon and thus more energy is required to cause the martensitic transformation in a filmy retained austenite. This morphology of retained austenite undergoes gradually to martensitic transformation, which in turn increases the toughness of the steel. Blocky shape of retained austenite transform into untampered martensite under an applied stress would be detrimental to toughness.

**Figure 6** OM image of microstructure of CS tempered at, (a) 100°C (b) 150°C (c) 200°C (d) 250°C (see online version for colours)

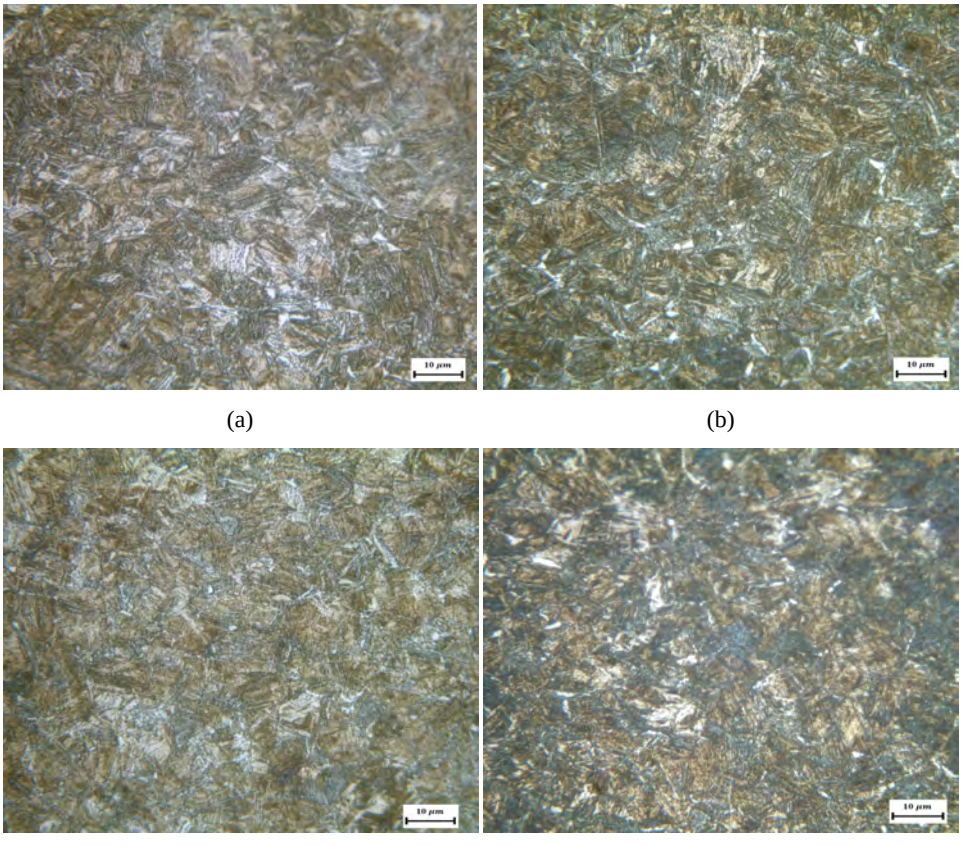

(a) (b)

(c) (d)

**Figure 7** OM image of microstructure of CNS tempered at, (a) 100°C (b) 150°C (c) 200°C (d) 250°C (see online version for colours)

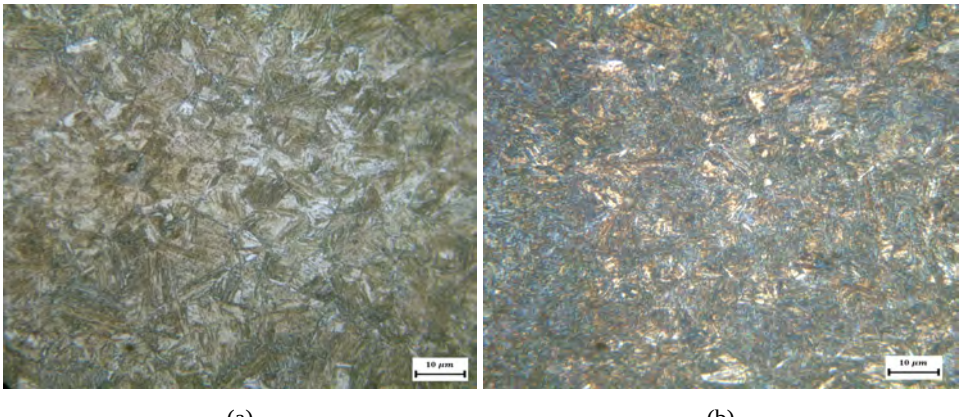

(a) (b)

**Figure 7** OM image of microstructure of CNS tempered at, (a) 100°C (b) 150°C (c) 200°C (d) 250°C (continued) (see online version for colours)

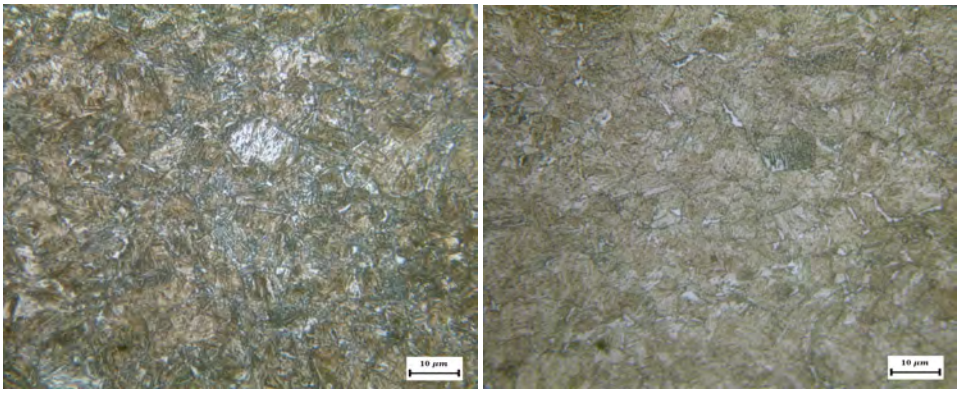

(c) (d)

**Table 3** Microstructure parameters of the CS and CNS achieved from image analysing software and XRD pattern analysis

| *Tempering temperature (°C)* | *Details of microstructure of CS* | *Details of microstructure of CNS* |
|---|---|---|
| 100 | Tempered martensite + 5% retained austenite | Tempered martensite + 5% retained austenite |
| 150 | Tempered martensite + 5% retained austenite | Tempered martensite + 5% retained austenite |
| 200 | Tempered martensite + 10% retained austenite | Tempered martensite + 10% retained austenite |
| 250 | Tempered martensite + 20% retained austenite | Tempered martensite + 20% retained austenite |

**Figure 8** Variations of volume fraction of retained austenite with tempering temperature of CS and CNS

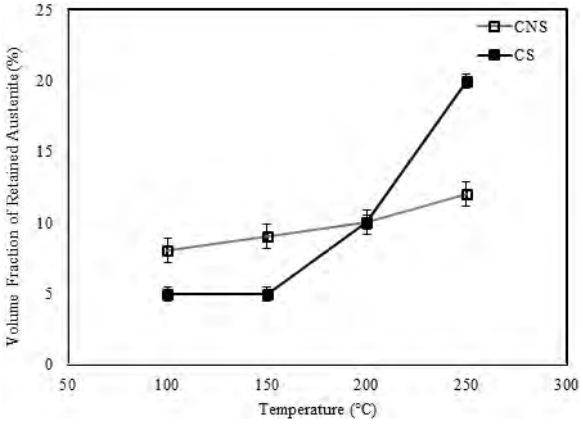

Volume fractions of tempered martensite and retained austenite were measured by using image analysing software and X-ray diffraction (XRD) pattern analysis and the data are summarised in Table 3. It can be claimed that the volume fractions of tempered martensite and retained austenite are similar in the CS and CNS. As mentioned earlier, austenite as a more ductile phase compared to tempered martensite consisting of two shape of blocky and filmy austenite, it can be predicated that higher austenite volume fraction in the microstructure, certainly, cannot lead to higher toughness of the steel. Therefore, an intermediate amount of retained austenite, which is mainly film austenite, will improve the mechanical properties. Variations of volume fraction of retained austenite with tempering temperature has been shown in Figure 8.

### *3.2 Impact toughness of CS and CNS*

In the Charpy impact test method, the specimen is momentarily subjected to very high energy by the impact of a heavy hammer under a dynamic loading condition, and the energy absorbed in the specimen contains both initiation and propagation energies of a crack initiated from a V-shaped notch (Kim et al., 2013).

Figure 9 shows the Charpy impact test results as a function of tempering temperature after different surface treatments. The Charpy impact energy increases as the tempering temperature increases, and then reaches a peak at 200°C and after that decreasing has been occurred, as shown in the figure. Also, the maximum amount of impact energy is obtained 13 and 21 J for samples of CS and CNS tempered at 200°C, respectively. Thus, the importance of tempering temperatures is increasing the toughness values of the samples. Charpy impact energy of the CNS is higher than that of the CS, which could be reasonably explained by the lower hardness distribution of CNS. In general, the impact toughness is proportional to the hardness of material, that is, the higher the hardness of the material is, the lower impact toughness.

**Figure 9** Variations of impact toughness energy as a function of tempering temperatures for CS and CNS

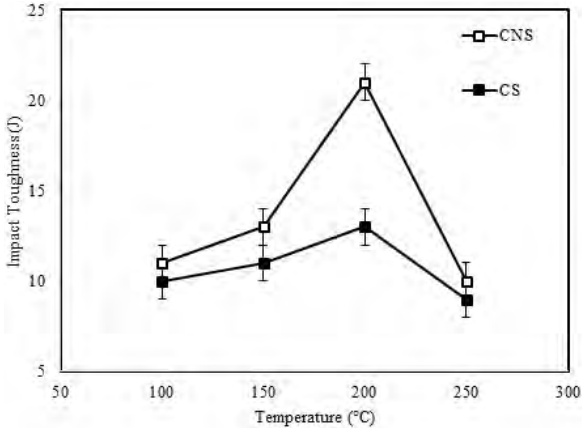


As shown in the figure, Charpy impact energy of the CNS is higher by about 60% than that of the CS tempered at 200°C, which shows the opposite trend of hardness. Also, thin

thickness and similar microstructure has been achieved in the CS and CNS which can be lead to the decreased spacing between cracks or void initiation sites.

The figure also indicates the increased impact energy about 45% and 110% with increasing tempering temperature from 100 to 200°C for CS and CNS, respectively. This implies that CNS have shown a high degree of impact energy increasing than CS. Moreover, the temperature required for achieve peak of impact toughness energy is 200°C for CS and CNS. Occurrence of the highest impact toughness in the samples transformed at 200°C can be as compound results of hardness and microstructure properties of the samples. Distribution of the retained austenite especially filmy shape austenite as a softer phase has a considerable effect on crack blunting and crack closure due to the compression caused by dilatation due to phase transformation. Therefore, samples tempered at 200°C, has shown higher impact toughness.

### *3.3 Fatigue behaviour of the CS and CNS*

According to the early section, maximum of the Charpy impact energy has been achieved of the CS and CNS tempered at 200°C. Fatigue fracture maximum load of the CS + tempered at 200°C, CNS + tempered at 200°C and untreated 16MnCr5 steel were measured, and the data are summarised in Table 4. It can be seen that, lower stress level or longer life are accordance with each other. It is obvious that, with increasing of number of cycles, level of stress decreasing has been occurred. The surface treatments have increased the fatigue strength with respect to the untreated 16MnCr5 steel. The fatigue strength of the untreated steel was equal to 390 MPa, while that of the CNS increased up to 750 MPa; a further increase up to 810 MPa was obtained for the CS at the 500,000 cycle number. Fatigue strength enhancement can be related to the high surface hardness and probably also to the high compressive residual stresses resulted from the surface treatment in the hardened layer. Fractography features near the fracture origin of the specimens without surface treatment showed that crack nucleation occurred at the specimen surfaces, while crack nucleation in the CS and CNS occurred at the interface between the hardened layer and the substrate surface. Also, slightly high fatigue strength of CS rather to the CNS, could be reasonably explained by the low hardness of CNS. Calculation of the actual loads acting on the spindle has shown that acting load in the tool by the workpiece is very low compared to the CNS fatigue strength. Therefore, relatively low fatigue strength of CNS would not be a significant limitation of this substitution.

**Table 4** Number of cycles to fatigue fracture of CS, CNS and untreated 16MnCr5 steel

| Number of cycles to fatigue fracture (Nf) | 10,000 | 100,000 | 500,000 |
|---|---|---|---|
| Maximum load for CS tempered at 200°C (MPa) | 960 | 865 | 810 |
| Maximum load for CNS tempered at 200°C (MPa) | 915 | 815 | 750 |
| Maximum load for untreated 16MnCr5 steel (MPa) | 600 | 465 | 390 |

In the lower stress level or longer life region, the crack's growth stage is a dominant factor in determining of the fatigue life. Depending on the depth of the surface treatments and its effect on the hardened layer of the samples, it can be claimed that crack propagation of fatigue fracture is affected by surface treatment. At low stress level, the factor of fatigue fracture controller is the crack initiation. Therefore, material with higher surfaces hardness, have a longer fatigue life. According to the relatively high difference

in fatigue strength of the surface treated and untreated samples at low stress levels, it can be concluded that surface treatment has the large effect on the stage of initiation of fatigue crack. Also, the surface region shows the higher fatigue strength than the centre region, because of higher hardness and compressive residual stress.

**Table 5** Surface roughness ($R_a$ and $R_z$) values of CS and CNS

| *Sample* | $R_a$ *(μm)* | $R_z$ *(μm)* |
|---|---|---|
| CS | 1.82 ± 0.12 | 7.95 ± 0.6 |
| CNS | 1.92 ± 0.22 | 9.52 ± 1.11 |

**Figure 10** Typical SEM of fracture surface of impact samples, (a) (b) CS tempered at 100°C (c) (d) CNS tempered at 100°C

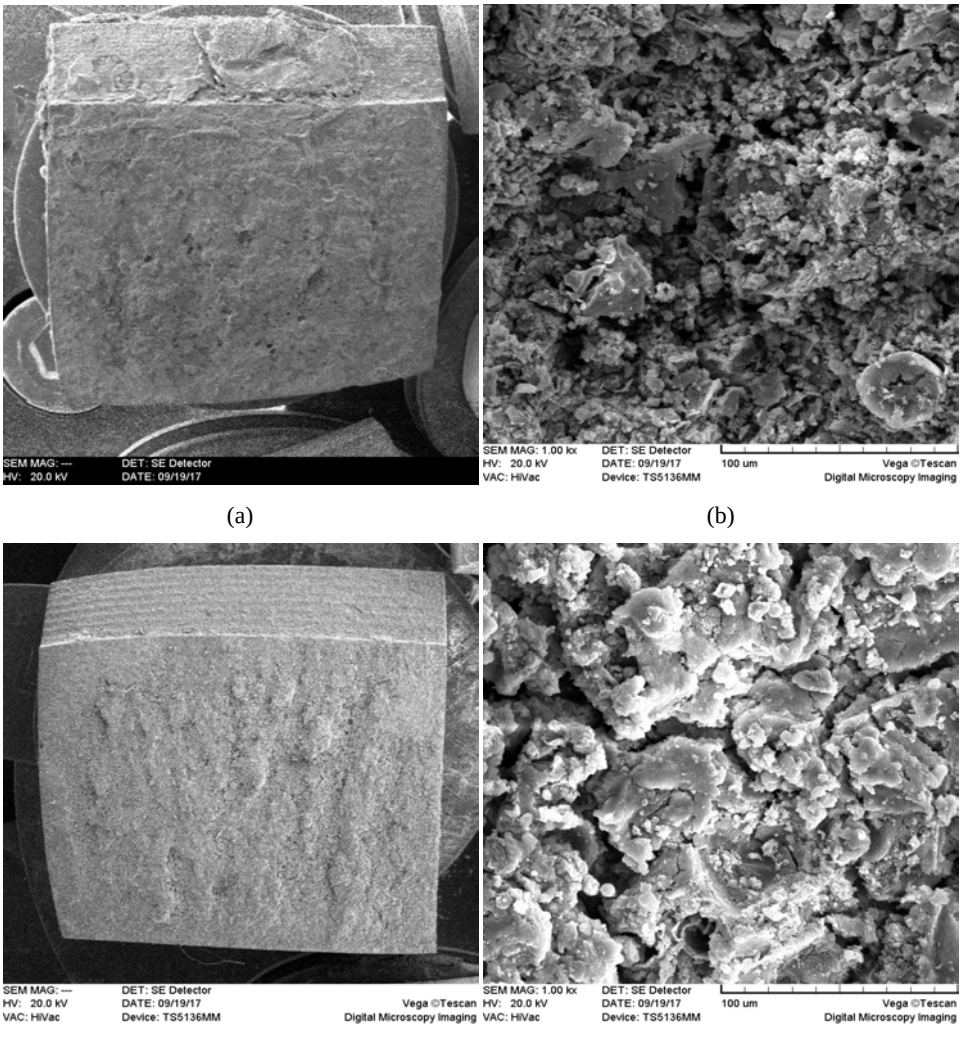

Since the surface quality of the sub-axis of the spindle can affect the machining accuracy, the average roughness ($R_a$) and ten-point parameter of roughness ($R_z$) values for each surface treated samples were measured by using MAHRTM. Table 5 is a statistical summary of the calculated $R_a$ and $R_z$ values. The mean $R_a$ and mean $R_z$ values of CNS were increased compared to the CS. This implies that surface roughness of the CNS is higher since this can be related to the growth of $\varepsilon$-nitrides on the surface of the CNS (Badisch et al., 2016), which lead to higher surface roughness.

### *3.4 Fractography of CS and CNS*

SEM analyses of fractured surface after the impact toughness test are shown in Figures 10 and Figure 11. The surface features clearly show that the mode of fracture changed from brittle at low temperature to ductile at high temperature. The cleavage fracture mode is mainly observed throughout the whole specimen, but some ductile dimpled fracture mode is also found in the fracture surfaces. Therefore, the fracture mode can be considered as quasi-cleavage fracture. Also, quasi-cleavage fracture appearance is dominantly displayed in the hardened surface layer. The lower quasi-cleavage fracture in CNS is obvious compared to the CS. This supports the increased impact energy in the CNS. The hardness of the CS is higher than that of the CNS; while opposite trend of Charpy impact energy has been achieved. These are responsible for higher quasi-cleavage fracture of CS.

**Table 6** Summary of the microstructural features and mechanical properties of CS and CNS

| *Index* | *Carburised specimens (CS)* | *Carbonitrided specimens (CNS)* | *Description* |
|---|---|---|---|
| Hardness number (HRC) | 57 | 56 | - |
| Depth of hardened layer (mm) | 0.83 | 0.5 mm | - |
| Microstructural feature | Tempered martensite + 10% retained austenite | Tempered martensite + 10% retained austenite | - |
| Charpy impact energy (J) | 13 | 21 | - |
| Fatigue strength at 500,000 cycles (MPa) | 810 | 750 | - |
| $R_a$ (μm) | 1.82±0.12 | 1.92±0.22 | - |
| How to fracture | Quasi-cleavage fracture | Quasi-cleavage fracture with some ductile dimples | - |
| Weight loss after 40 min wear (gr) | 0.0132 | 0.005 | Yoozbashi and Almasi (2018) |

Summary of the microstructural features and mechanical properties of CS and CNS have been shown in the Table 6. The CS and CNS are relatively similar in the properties such as hardness, microstructure features, and how to fracture while show a difference in the properties such as hardness distribution, depth of hardened layer, Charpy impact energy, roughness and wear properties which achieved in the Yoozbashi et al. (2017) study. It is important to be noted that due to the lower temperature required for the carbonitriding, compared to the carburising, distortion during treatment will be deceased.

**Figure 11** Typical SEM of fracture surface of impact samples, (a) (b) CS tempered at 250°C (c) (d) CNS tempered at 200°C

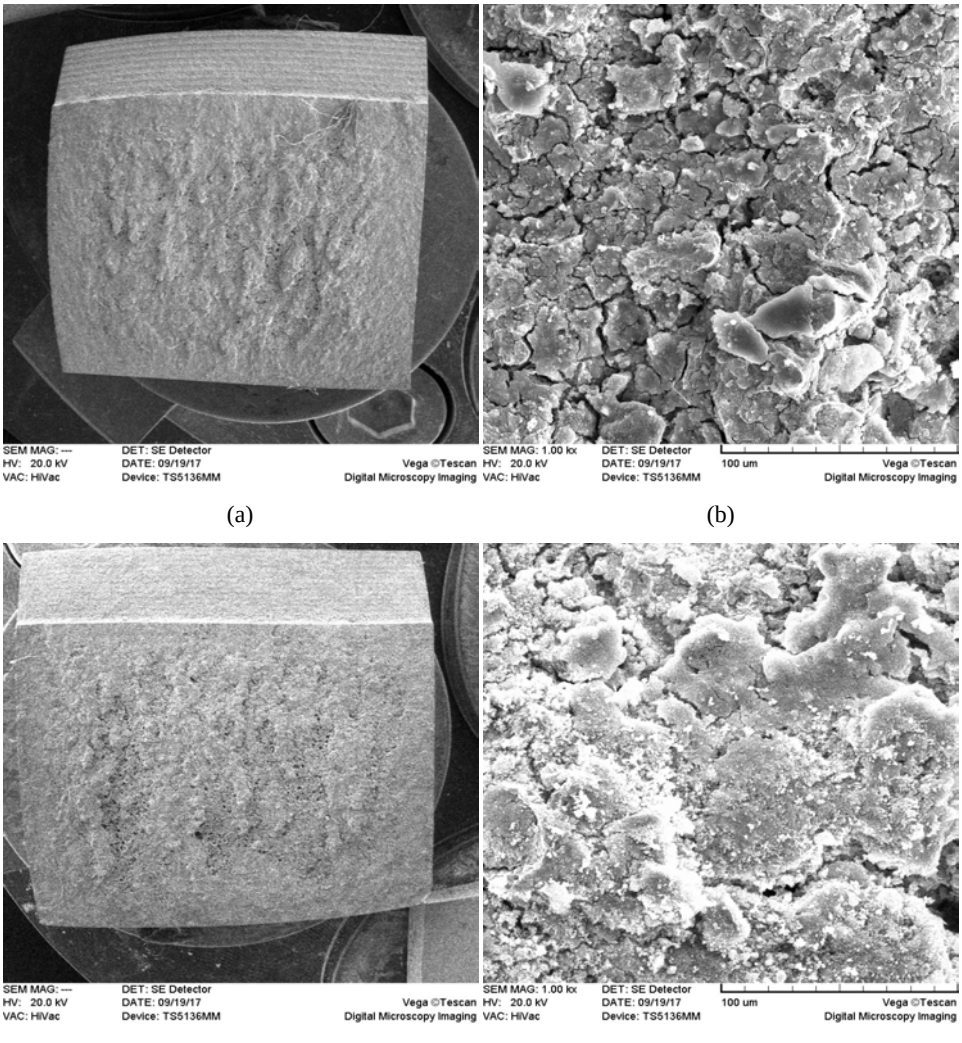


## 4 Conclusions

- Charpy impact energy of the CNS is higher than that of the CS, as a result of lower hardness distribution of CNS and retained austenite effects in the microstructure.
- Impact energy enhancement is about 45% and 110% with increasing tempering temperature from 100 to 200°C for CS and CNS, respectively.
- The sum of the loads that the spindle endurances during machining is less than the fatigue strength obtained through experimental tests. Therefore, relatively low

fatigue strength of CNS compared to the CS would not be a significant limitation of this substitution.

- A possible explanation for of surface roughness increasing during carbonitriding can be related to the growth of $\varepsilon$-nitrides on the surface of specimens.
- Considering all the above items, substitution of carburised 16MnCr5 used in sub-axis of machine tool spindle by carbonitrided 16MnCr5 steel is recommended.

## References

Abele, E., Altintas, Y. and Brecher, C. (2010) 'Machine tool spindle units', *CIRP Annals*, Vol. 59, No. 2, pp.781–802 [online] https://doi.org/10.1016/j.cirp.2010.05.002.

Altintas, Y. and Cao, Y. (2005) 'Virtual design and optimization of machine tool spindles', *CIRP Annals*, Vol. 54, No. 1, pp.379–382 [online] https://doi.org/10.1016/S0007-8506(07)60127-9.

American Society for Testing and Materials (2013) *ASTM E23-12c: Standard Test Methods for Notched Bar Impact Testing of Metallic Materials* [online] https://mmplab.um.ac.ir/images/248/standard/impact/E23_12c_Standard_Test_Methods_for.pdf.

Badisch, E., Trausmuth, A., Rodríguez Ripoll, M., Diem, A., Kunze, W., Glück, J., Lingenhöle, K. and Orth, P. (2016) 'Influence of nitrocarburizing process parameters on the development of surface roughness and layer formation', in *Key Engineering Materials*, Trans Tech Publications Ltd., Vol. 674, pp.325–330 [online] https://doi.org/10.1016/j.wear.2018.05.021.

Brecher, C., Spachtholz, G. and Paepenmüller, F. (2007) 'Developments for high performance machine tool spindles', *CIRP Annals*, Vol. 56, No. 1, pp.395–399 [online] https://doi.org/10.1016/j.cirp.2007.05.092.

Cao, Y. and Altintas, Y. (2007) 'Modeling of spindle-bearing and machine tool systems for virtual simulation of milling operations', *International Journal of Machine Tools and Manufacture*, Vol. 47, No. 9, pp.1342–1350 [online] https://doi.org/10.1016/j.ijmachtools.2006.08.006.

Ceschini, L. and Minak, G. (2008) 'Fatigue behaviour of low temperature carburised AISI 316L austenitic stainless steel', *Surface and Coatings Technology*, Vol. 202, No. 9, pp.1778–1784 [online] https://doi.org/10.1016/j.surfcoat.2007.07.066.

Dastmozd, N., Eshagh Beigi, A. and Ashrafizadeh, F. (2014) 'Hardening of 16MnCr5 and Ck45 (in Persian)', Paper presented at *8th National Congress on Agr. Machinery Eng. (Biosystem) and Mechanization*, Mashahd, Iran, 29–30 June [online] https://civilica.com/doc/284420/.

Davis, J.R. (2002) *Surface Hardening of Steels: Understanding the Basics*, ASM International [online] https://www.asminternational.org/search/journal_content/56/10192/06952G/PUBLICATION.

DIN 50 113 (2018) *Rotating Bar Bending Fatigue Test*, German Standards Organization [online] https://www.boutique.afnor.org/en-gb/standard/din-50113/testing-of-metallic-materials-rotating-bar-bending-fatigue-test/eu155427/180734.

Farrahi, G.H. and Ghadbeigi, H. (2006) 'An investigation into the effect of various surface treatments on fatigue life of a tool steel', *Journal of Materials Processing Technology*, Vol. 174, Nos. 1–3, pp.318–324 [online] https://doi.org/10.1016/j.jmatprotec.2006.01.014.

Forrest, P.G. (2013) *Fatigue of Metals*, Elsevier [online] https://www.elsevier.com/books/fatigue-of-metals/forrest/978-0-08-009729-9.

Hertzberg, R.W., Vinci, R.P. and Hertzberg, J.L. (2020) *Deformation and Fracture Mechanics of Engineering Materials*, John Wiley & Sons [online] https://www.wiley.com/en-us/Deformation+and+Fracture+Mechanics+of+Engineering+Materials%2C+5th+Edition-p-9780470527801.

Kim, H., Kang, M., Jung, H.J., Kim, H.S., Bae, C.M. and Lee, S. (2013) 'Mechanisms of toughness improvement in Charpy impact and fracture toughness tests of non-heat-treating cold-drawn steel bar', *Materials Science and Engineering: A*, Vol. 571, pp.38–48 [online] https://doi.org/10.1016/j.msea.2013.02.011.

Krauss, G. (2015) *Steels: Heat Treatment and Processing Principles*, ASM International, p.497 [online] https://www.asminternational.org/documents/10192/1849770/05441G_TOC.pdf/3298a867-3fe5-49ad-bc00-9bce6dcc2dc1.

Li, H. and Shin, Y.C. (2004) 'Analysis of bearing configuration effects on high speed spindles using an integrated dynamic thermo-mechanical spindle model', *International Journal of Machine Tools and Manufacture*, Vol. 44, No. 4, pp.347–364 [online] https://doi.org/10.1016/j.ijmachtools.2003.10.011.

Mohan, N. and Arul, S. (2018) 'Effect of cryogenic treatment on the mechanical properties of alloy steel 16MnCr5', *Materials Today: Proceedings*, Vol. 5, No. 11, pp.25265–25275 [online] https://doi.org/10.1016/j.matpr.2018.10.329.

Oropeza, C. (2002) *A New Approach to Evaluate Fracture Strength of UV-LIGA Fabricated Nickel Specimens* [online] https://digitalcommons.lsu.edu/cgi/viewcontent.cgi?article=3668&context=gradschool_theses.

Putatunda, S.K. (2001) 'Fracture toughness of a high carbon and high silicon steel', *Materials Science and Engineering: A*, Vol. 297, Nos. 1–2, pp.31–43 [online] https://doi.org/10.1016/S0921-5093(00)01272-7.

Sirin, S.Y., Sirin, K. and Kaluc, E. (2008) 'Effect of the ion nitriding surface hardening process on fatigue behavior of AISI 4340 steel', *Materials Characterization*, Vol. 59, No. 4, pp.351–358 [online] https://doi.org/10.1016/j.matchar.2007.01.019.

Tchankov, D.S. and Dimitrov, D.I. (2000) 'Fatigue strength of ion nitrided steel specimens', *International Journal of Materials and Product Technology*, Vol. 15, Nos. 1–2, pp.1–9.

Winck, L.B., Ferreira, J.L.A., Araujo, J.A., Manfrinato, M.D. and Da Silva, C.R.M. (2013) 'Surface nitriding influence on the fatigue life behavior of ASTM A743 steel type CA6NM', *Surface and Coatings Technology*, Vol. 232, pp.844–850 [online] https://doi.org/10.1016/j.surfcoat.2013.06.110.

Yeğen, İ. and Usta, M. (2010) 'The effect of salt bath cementation on mechanical behavior of hot-rolled and cold-drawn SAE 8620 and 16MnCr5 steels', *Vacuum*, Vol. 85, No. 3, pp.390–396 [online] https://doi.org/10.1016/j.vacuum.2010.07.013.

Yoozbashi, M.N. and Almasi, A. (2018) 'The effect of various surface heat treatments on wear behavior of 16MnCr5 steel used in spindles axis of machine tools', *Journal of Mechanical Engineering*, Vol. 48, No. 1, pp.351–357 [online] https://tumechj.tabrizu.ac.ir/article_7512.html.

Yoozbashi, M.N. Vahedi, N. and Almasi, A. (2017) 'The effects of tempering temperature on wear behavior of AISI 5115 steel used in spindles of machine tools', *Journal of Mechanical Engineering*, Vol. 47, No. 3, pp.297–305 [online] https://tumechj.tabrizu.ac.ir/article_6763.html.

Zhang, Z., Lin, P., Zhou, H. and Ren, L. (2013) 'Microstructure, hardness, and thermal fatigue behavior of H21 steel processed by laser surface remelting', *Applied Surface Science*, Vol. 276, pp.62–67 [online] https://doi.org/10.1016/j.apsusc.2013.03.009.